Type-2 Fuzzy Broad Learning System

Honggui Han, *Senior Member, IEEE*, Zheng Liu, Hongxu Liu, Junfei Qiao, *Member, IEEE*, and C. L. Philip Chen, *Fellow, IEEE*

***Abstract*—The broad learning system (BLS) has been identified as an important research topic in machine learning. However, the typical BLS suffers from poor robustness for uncertainties because of its characteristic of the deterministic representation. To overcome this problem, a type-2 fuzzy BLS (FBLS) is designed and analyzed in this article. First, a group of interval type-2 fuzzy neurons was used to replace the feature neurons of BLS. Then, the representation of BLS can be improved to obtain good robustness. Second, a fuzzy pseudoinverse learning algorithm was designed to adjust the parameter of type-2 FBLS. Then, the proposed type-2 FBLS was able to maintain the fast computational nature of BLS. Third, a theoretical analysis on the convergence of type-2 FBLS was given to show the computational efficiency. Finally, some benchmark and practical problems were used to test the merits of type-2 FBLS. The experimental results indicated that the proposed type-2 FBLS can achieve outstanding performance.**

***Index Terms*—Broad learning system (BLS), fuzzy pseudoinverse learning (FPL) algorithm, interval type-2 fuzzy neuron, robustness.**

I. Introduction

THE BROAD learning system (BLS), which has been considered as an important machine-learning algorithm, has gained much attention in recent years and has numerous applications, for example, dynamic pattern recognition [1], the nonlinear regression analysis [2], the time-series prediction [3], and so on [4]. Without stacking the layer-structure, BLS, taking the advantage of the flatted structure [5], is a very fast and efficient discriminative learning method in the big data environment [6]. However, due to the frequent existence of nonlinearities and uncertainties in modern processes [7], how to ensure satisfactory robustness poses nontrivial challenges to typical BLS [8].

In order to improve the robustness of BLS, Jin and Chen designed a regularized robust BLS (RR-BLS) in [9]. For RR-BLS, a regularization term was used to make the weight to be sparse to mitigate the effect of uncertainties. Then, the robust performance of RR-BLS was able to improve a lot compared with the standard BLS. Meanwhile, a weighted BLS (WBLS), where a weighted penalty factor was assigned to reduce the impact of uncertainties, was developed for modeling the industrial process [10]. A robust manifold BLS (RM-BLS), where a random manifold feature selection was used to estimate the external uncertainties, was proposed for the chaotic time-series prediction [11]. The simulation results illustrated that both WBLS and RM-BLS can achieve better performance in terms of generalization and robustness than the traditional BLS. However, it is difficult to obtain the mathematical formula or the process model for these above improved BLSs to design the additional terms for tackling the uncertainties [12].

Recently, the fuzzy method has been considered as a promising strategy to deal with the uncertainties with easy implementation [13] and good robustness [14]. For example, a wavelet type-1-fuzzy neural network (WT1FNN) was developed for nonlinear systems [15], in which a wavelet-function was introduced. Feng and Chen [16] presented a fuzzy BLS (FBLS) to handle the uncertainties for regression and classification problems. In this FBLS, the feature neurons of standard BLS were replaced by the Takagi–Sugeno fuzzy systems. Moreover, in order to verify the robust performance of FBLS in real applications, this FBLS was used to synthesize the high dynamic range images with the uncertainties in [17]. The results indicated that the FBLS can obtain better robust performance than some other methods. Furthermore, an improved BLS based on the TSK fuzzy system (TSK-FBLS) was established for nonlinear system identification in [18]. For TSK-FBLS, the TSK fuzzy system was used to substitute the feature neurons of BLS to deal with the uncertainties. The simulation results demonstrated that this TSK-FBLS can obtain good robust performance and prediction accuracy. However, since there may exist not only system nonlinearities but also the parametric uncertainties, one of the main drawbacks of these advanced FBLSs is that the precise and crisp membership grades of the type-1-fuzzy set (T1-FS) result in the deficiency of interpretability for uncertainties [19].

The interval type-2 fuzzy set (IT2-FS), which can deal with both of the system nonlinearities and parametric uncertainties by considering lower and upper membership functions and relative weighting functions [20], has been used to improve the

Manuscript received 19 September 2020; revised 22 January 2021 and 30 March 2021; accepted 30 March 2021. Date of publication 22 April 2021; date of current version 16 September 2022. This work was supported in part by the National Key Research and Development Project under Grant 2018YFC1900800-5; in part by the National Science Foundation of China under Grant 61890930-5, Grant 62021003, and Grant 61903010; in part by the Beijing Outstanding Young Scientist Program under Grant BJJWZYJH01201910005020; and in part by the Beijing Natural Science Foundation under Grant KZ202110005009. This article was recommended by Associate Editor E. Herrera-Viedma. *(Corresponding author: Honggui Han.)*

Honggui Han, Zheng Liu, Hongxu Liu, and Junfei Qiao are with the Faculty of Information Technology, Beijing Key Laboratory of Computational Intelligence and Intelligent System, Engineering Research Center of Digital Community, Ministry of Education, Beijing Artificial Intelligence Institute and Beijing Laboratory for Urban Mass Transit, Beijing University of Technology, Beijing 100124, China (e-mail: rechardhan@sina.com).

C. L. Philip Chen was with the Faculty of Science and Technology, the University of Macau, Macau SAR 99999, China. He is now with the School of Computer Science and Engineering, South China University of Technology, Guangzhou 510006, China (e-mail: philip.chen@ieee.org).

Color versions of one or more figures in this article are available at https://doi.org/10.1109/TCYB.2021.3070578.

Digital Object Identifier 10.1109/TCYB.2021.3070578

interpretability for uncertain problems [21]. Eyoh *et al.* introduced an interval type-2 fuzzy neural network (IT2FNN) to deal with the parametric uncertainties in [22]. The results indicated that the IT2FNN method can obtain better interpretable and robust performance than type-1 FNNs. Lin *et al.* [23] designed a function-link IT2FNN (FIT2FNN) for nonlinear system identification. The function-link mechanism can enhance the interpretable performance of IT2FNN to obtain an accurate approximation of uncertainties. The results revealed that this FIT2FNN can achieve better performance than the IT2FNN [22] in terms of model interpretability and robustness. However, the above methods focused much on designing the structure of IT2FNN but not the parameter adjustment. Han *et al.* [24] designed an adaptive second-order algorithm to optimize the parameter of IT2FNN. The adaptive second-order learning algorithm can optimize both the nonlinear parameter and learning rate simultaneously. The experimental results illustrated that the proposed algorithm can improve the learning performance for modeling nonlinear systems with uncertainties. Moreover, a hybrid learning method (HLM), based on the gradient descent and extended Kalman filter, was introduced to update the parameter of IT2FNN in [25]. In this HLM, the gradient descent method was developed to adjust the antecedents part, and the extended Kalman filter was used to update the consequent parameter. The results revealed that this HLM was able to obtain better learning performance than other methods. Moreover, there are some other algorithms to optimize the parameters of IT2FNN based on genetic algorithm [26], particle swarm optimization [27], etc. [28]. However, these above algorithms lead to a heavy computational burden in the learning process [29]. Therefore, the interpretability of IT2-FS for uncertainty problems motivates our attempt to integrate it with BLS and design a novel FBLS model. Moreover, how to obtain an efficient learning algorithm to improve the robustness of FBLS for uncertainties is still an open issue [30].

Motivated by the above analysis and review, a type-2 FBLS (T2F-BLS), including a set of interval type-2 fuzzy neurons and a fuzzy pseudoinverse learning (FPL) algorithm, is proposed in this article. The major contributions of T2F-BLS contain the following parts.

1) The interval type-2 fuzzy neurons are introduced to enhance the representation of BLS to deal with the system nonlinearities and parametric uncertainties. Therefore, the proposed T2F-BLS can reduce the impact of uncertainties to obtain good robust performance in the learning process.
2) A novel FPL algorithm is developed to adjust the parameter of T2F-BLS with fast computation. Therefore, the learning performance of T2F-BLS can be improved to strengthen the robustness for uncertainties.
3) The convergence of T2F-BLS has been demonstrated theoretically and experimentally. Therefore, the proposed T2F-BLS can ensure its successful applications.
4) The proposed T2F-BLS is applied for the prediction of nonlinear systems with uncertainty. The experimental results demonstrate the superiority and efficacy of T2F-BLS.

The remainder of this article is organized as follows. The concept of BLS and IT2-FS is briefly described in Section II. In Section III, the proposed T2F-BLS, including the structure of T2F-BLS and the FPL algorithm, is discussed in detail. Moreover, the convergence of T2F-BLS is also analyzed. The experimental results of a popular benchmark and some practical problems are presented in Section IV. The results demonstrate that this proposed T2F-BLS can achieve better robustness, higher accuracy, and faster computation than some existing methods. Finally, Section V gives some conclusions.

II. Problem Formulation

In this section, the traditional BLS is presented based on the functional-link network and ridge regression algorithm [31]. After that, a brief introduction of IT2-FS is given.

A. Broad Learning System

BLS is an improved flat network, which consists of four main parts: 1) the input; 2) the feature neurons; 3) the enhancement neurons; and 4) the output. Based on the results in [32], the output of BLS is

$$\mathbf{Y}(t) = [\mathbf{Z}(t)|\mathbf{H}(t)]\mathbf{W}(t) \tag{1}$$

where

$$\mathbf{Z}(t) = [\mathbf{z}_1(t), \ldots, \mathbf{z}_i(t), \ldots, \mathbf{z}_n(t)],\ i = 1, 2, \ldots, n \tag{2}$$

$$\mathbf{H}(t) = \left[\mathbf{h}_1(t), \ldots, \mathbf{h}_j(t), \ldots, \mathbf{h}_m(t)\right],\ j = 1, 2, \ldots, m \tag{3}$$

where $\mathbf{z}_i(t)$ is the output of the ith group feature neurons and $\mathbf{h}_j(t)$ is the output of the jth group enhancement neuron

$$\mathbf{z}_i(t) = \phi_i\big(\mathbf{X}(t)\mathbf{w}_{ei}(t) + \boldsymbol{\beta}_{ei}(t)\big) \tag{4}$$

$$\mathbf{h}_j(t) = \xi_j\big(\mathbf{Z}(t)\mathbf{w}_{hj}(t) + \boldsymbol{\beta}_{hj}(t)\big) \tag{5}$$

where $\varphi_i()$ is the feature mapping and $\xi_j()$ is a tanh function. $\mathbf{X}(t)$ is the input of BLS, $\mathbf{w}_{ei}(t)$ and $\boldsymbol{\beta}_{ei}(t)$ are the weight and bias terms connecting the input to the feature neurons, $\mathbf{w}_{hj}(t)$ and $\boldsymbol{\beta}_{hj}(t)$ are the weight and bias term connecting the output of feature neurons to the enhancement neurons, and $\mathbf{W}(t)$ is the output weight connecting the feature neurons and the enhancement neurons to the output neurons

$$\mathbf{W}(t) = \mathbf{D}_{ZH}(t)^{+}\bar{\mathbf{Y}}(t) \tag{6}$$

$$\mathbf{D}_{ZH}(t)^{+} = \lim_{\lambda \to 0}\left[(\mathbf{D}_{ZH}(t))^T\mathbf{D}_{ZH}(t) + \lambda\mathbf{I}\right]^{-1}(\mathbf{D}_{ZH}(t))^T \tag{7}$$

$$\mathbf{D}_{ZH}(t) = [\mathbf{Z}(t), \mathbf{H}(t)] \tag{8}$$

where $\mathbf{D}_{ZH}(t)$ is the expanded matrix, $\bar{\mathbf{Y}}(t)$ is the real output, λ is a positive constant, and $\mathbf{I}$ is an identity matrix.

B. Interval Type-2-Fuzzy Set

A T2-FS can be described as

$$\mathbf{A}(t) = \{((x(t), u(t)), \mu(x(t), u(t)))|\ \forall x(t) \in \mathbf{U}(t) \quad \forall u(t) \in \mathbf{J}(t) \subseteq [0, 1], 0 \le \mu(x(t), u(t)) \le 1\} \tag{9}$$

where $x(t)$ is the input, $u(t)$ is the secondary variable of T2-FS, $\mu(x(t),u(t))$ is the type-2 membership function, $\mathbf{U}(t)$ is a finite and nonempty set, and $\mathbf{J}(t)$ is the primary membership. When

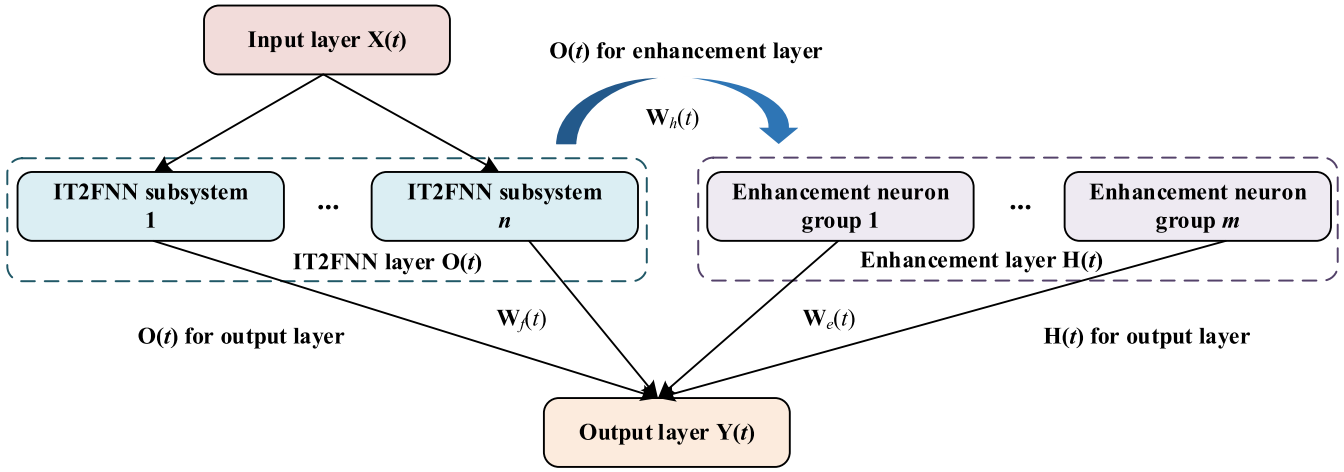

Fig. 1. Structure of T2F-BLS.

$\mu(x(t), u(t)) = 1$ in (9), $\mathbf{A}(t)$ is called an IT2-FS. It should be noted that the footprint of uncertainty is the important and complete description of IT2-FS [33]. The mathematical definition of footprint of uncertainty can be expressed as

$$\mathbf{f}(t) = \bigcup_{x(t)\in X(t)} \left[\underline{\mu}(x(t)), \bar{\mu}(x(t))\right] \tag{10}$$

where $\underline{\mu}(x(t))$ and $\bar{\mu}(x(t))$ are the lower and upper membership functions of the footprint of uncertainty, respectively. Thus, compared to T1-FS, IT2-FS is more suitable to deal with uncertain problems [34].

III. Type-2 Fuzzy Broad Learning System

For this T2F-BLS, both the structural design and parameter adjustment are considered in the learning process. In the structure design process, the interval type-2 fuzzy neurons are employed to replace the feature neurons of BLS. Meanwhile, a novel FPL algorithm is developed to update the parameter of T2F-BLS in the learning process. In addition, the convergence of T2F-BLS is given in detail.

A. Structure Design of the Type-2 Fuzzy Broad Learning System

To design a BLS with satisfactory robust performance, a T2F-BLS, based on a group of interval type-2 fuzzy neurons, is developed in this study (as shown in Fig. 1). From Fig. 1, it can be seen that this T2F-BLS is established in the form of a flat network, which contains the input layer, IT2FNN layer, enhancement layer, and output layer. The input layer is mapped into the IT2FNN layer. Then, the interval type-2 fuzzy neurons are sent into enhancement neurons for nonlinear transformation. Furthermore, the IT2FNN layer and enhancement layer are connected to the output layer, and the connection weight is the model parameter.

For a clear understanding of T2F-BLS, the mathematical function of each layer is described as follows.

Input Layer: The mathematical description of the input layer is $\mathbf{X}(t) = [\mathbf{x}_1(t), \mathbf{x}_2(t), \ldots, \mathbf{x}_P(t)]^T$, where $\mathbf{x}_p(t) = [x_1(t), x_2(t), \ldots, x_S(t)]$, $p = 1, 2, \ldots, P$. P is the number of samples and S is the number of neurons in this layer.

IT2FNN Layer: There are n IT2FNN subsystems in this layer. In each IT2FNN subsystem, the antecedent part is IT2-FS with uncertain means and fixed standard derivation. Meanwhile, the consequent part is explained by the type-reduction operation with interval weight. The rule in the ith IT2FNN subsystem is

$$R^q: \text{IF } x_1(t) \text{ is } A_{I1qi}(t) \text{ and} \ldots x_s(t) \text{ is } A_{Isqi}(t) \ldots \text{and } x_S(t) \text{ is } A_{ISqi}(t) \text{ THEN } f_{qi}(t) = N_{qi}(t) \tag{11}$$

where $s = 1, 2, \ldots, S$, $q = 1, 2, \ldots, Q$, Q is the number of rule neurons, $A_{Isqi}(t)$ is the type-2 fuzzy membership function for the qth rule neuron of the sth input neuron, and $N_{qi}(t)$ is the type-2 fuzzy membership function for the output of the qth rule neuron, the output of the IT2FNN layer is

$$\mathbf{O}(t) = [\mathbf{o}_1(t), \mathbf{o}_2(t), \ldots, \mathbf{o}_n(t)] \tag{12}$$

$$\mathbf{o}_i(t) = [o_{1i}(t), o_{2i}(t), \ldots, o_{Ki}(t)] \tag{13}$$

where $\mathbf{o}_i(t)$ is the output of the ith IT2FNN, K is the number of output neurons of the ith IT2FNN subsystem, $o_{ki}(t)$ is the output of the kth output neuron

$$o_{ki}(t) = \left(\underline{o}_{ki}(t) + \bar{o}_{ki}(t)\right)/2, k = 1, 2, \ldots, K \tag{14}$$

where $\underline{o}_{ki}(t)$ and $\bar{o}_{ki}(t)$ are lower bounded and upper bounded outputs of the kth consequent neuron

$$\underline{o}_{ki}(t) = \sum_{q=1}^{Q} \underline{f}_{qi}(t)\underline{w}_{qk}(t) \Big/ \sum_{q=1}^{Q} \underline{f}_{qi}(t) \tag{15}$$

$$\bar{o}_{ki}(t) = \sum_{q=1}^{Q} \bar{f}_{qi}(t)\bar{w}_{qk}(t) \Big/ \sum_{q=1}^{Q} \bar{f}_{qi}(t) \tag{16}$$

where $\underline{w}_{qk}(t)$ and $\bar{w}_{qk}(t)$ are lower bounded and upper bounded values of the interval weight between the kth consequent neuron and the qth firing neuron, $\underline{f}_{qi}(t)$ and $\bar{f}_{qi}(t)$ are the lower bounded and upper bounded outputs of the qth firing neuron, and the output of the qth firing neuron is

$$\mathbf{f}_{qi}(t) = \left[\underline{f}_{qi}(t), \bar{f}_{qi}(t)\right] \tag{17}$$

$$\underline{f}_{qi}(t) = \prod_{s=1}^{S} \underline{\mu}_{qsi}(t) \tag{18}$$

$$\bar{f}_{qi}(t) = \prod_{s=1}^{S} \bar{\mu}_{qsi}(t) \tag{19}$$

where $\underline{\mu}_{qsi}(t)$ and $\bar{\mu}_{qsi}(t)$ are lower bounded and upper bounded output values of the qth membership function neuron. In this study, the Gaussian membership function is employed to calculate the membership value. Then, the output of the qth membership function neuron is

$$\begin{aligned}\mu_{qsi}(t) &= \exp\left(-\frac{1}{2}\left(\left(x_s(t) - u_{qsi}(t)\right)/\sigma_{qsi}(t)\right)^2\right) \\ &= N\left(u_{qsi}(t), \sigma_{qsi}(t), x_s(t)\right)\end{aligned} \tag{20}$$

where $u_{qsi}(t) \in [\underline{u}_{qsi}(t), \bar{u}_{qsi}(t)]$ is the uncertain mean and $\sigma_{qsi}(t)$ is the fixed standard deviation.

Enhancement Layer: There are m groups of enhancement neuron in this layer. The output of the enhancement layer is

$$\mathbf{H}(t) = [\mathbf{h}_1(t), \mathbf{h}_2(t), \ldots, \mathbf{h}_m(t)] \tag{21}$$

$$\mathbf{h}_j(t) = \xi_j\left(\mathbf{O}(t)\mathbf{w}_{hj}(t) + \boldsymbol{\beta}_{hj}(t)\right),\ j = 1, 2, \ldots, m \tag{22}$$

where $\mathbf{h}_j(t) = [h_{1j}(t), h_{2j}(t), \ldots, h_{Lj}(t)]$ is the output of the jth group enhancement neuron, L is the number of neurons in the jth group enhancement neuron, and $\mathbf{W}_h(t) = [\mathbf{w}_{h1}(t), \mathbf{w}_{h2}(t), \ldots, \mathbf{w}_{hm}(t)]$ is the weight between the IT2FNN layer and the enhancement layer. $\mathbf{w}_{hj}(t) = [w_{hj1}(t), w_{hj2}(t), \ldots, w_{hjn}(t)]$ and $\boldsymbol{\beta}_{hj}(t) = [\beta_{hj1}(t), \beta_{hj2}(t), \ldots, \beta_{hjn}(t)]$ are the weight and bias between the IT2FNN layer and the jth group enhancement neuron.

Output Layer: There are C neurons in this layer. The output of the output layer is

$$\mathbf{Y}(t) = \mathbf{O}(t)\mathbf{W}_f(t) + \mathbf{H}(t)\mathbf{W}_e(t) \tag{23}$$

where $\mathbf{W}_f(t) = [\mathbf{w}_{f1}(t), \mathbf{w}_{f2}(t), \ldots, \mathbf{w}_{fC}(t)]$ is the weight vector between the IT2FNN layer and the output layer, and $\mathbf{W}_e(t) = [\mathbf{w}_{e1}(t), \mathbf{w}_{e2}(t), \ldots, \mathbf{w}_{eC}(t)]$ is the weight vector between the enhancement layer and the output layer.

Remark 1: In this T2F-BLS, the interval type-2 fuzzy neuron can improve the representation. Therefore, the structure design of T2F-BLS is able to enhance the robustness.

B. Fuzzy Pseudoinverse Learning Algorithm

In this T2F-BLS, an FPL algorithm is developed to update the output weights $\mathbf{W}_f(t)$ and $\mathbf{W}_e(t)$. To introduce the learning process of FPL clearly, the output of T2F-BLS can be rewritten as

$$\mathbf{Y}(t) = [\mathbf{O}(t), \mathbf{H}(t)]\begin{bmatrix}\mathbf{W}_f(t) \\ \mathbf{W}_e(t)\end{bmatrix} = \mathbf{D}(t)\mathbf{W}(t) \tag{24}$$

where $\mathbf{D}(t) = [\mathbf{O}(t), \mathbf{H}(t)]$ and $\mathbf{W}(t) = [\mathbf{W}_f(t), \mathbf{W}_e(t)]^T$. Then, the output weight $\mathbf{W}(t)$ is

$$\begin{aligned}\mathbf{W}(t) &= \underset{W}{\operatorname{argmin}}\left(\eta(t)\left\|\mathbf{Y}(t) - \bar{\mathbf{Y}}(t)\right\| + \|\mathbf{W}(t)\|^2\right) \\ &= \underset{W}{\operatorname{argmin}}\left(\eta(t)\left\|\mathbf{D}(t) - \mathbf{W}(t) - \bar{\mathbf{Y}}(t)\right\| + \|\mathbf{W}(t)\|^2\right)\end{aligned} \tag{25}$$

where $\bar{\mathbf{Y}}(t)$ is the real output and $\eta(t)$ is the adaptive learning rate

$$\eta(t) = \lambda(t)\eta(t-1) \tag{26}$$

$$\lambda(t) = \left(\tau^{\min}(t) + \lambda(t-1)\right)\Big/\left(\tau^{\max}(t) + 1\right) \tag{27}$$

where $\tau^{\max}(t)$ and $\tau^{\min}(t)$ are the maximum and minimum eigenvalues of $\mathbf{D}(t)^T\mathbf{D}(t)$, respectively, $(0<\eta(t)<1)$. Then, the output weight $\mathbf{W}(t)$ can be calculated as

$$\mathbf{W}(t) = \left(\mathbf{D}(t)^T\mathbf{D}(t) + \eta(t)\mathbf{I}\right)^{-1}\mathbf{D}(t)^T\bar{Y}(t) = \mathbf{Q}(t)^{-1}\boldsymbol{\Psi}(t) \tag{28}$$

where $\mathbf{Q}(t) = \mathbf{D}(t)^T\mathbf{D}(t) + \eta(t)\mathbf{I}$ and $\boldsymbol{\Psi}(t) = \mathbf{D}(t)^T\bar{\mathbf{Y}}(t)$. Thus, the output weight $\mathbf{W}(t+1)$ is updated as

$$\mathbf{W}(t+1) = \mathbf{Q}(t+1)^{-1}\boldsymbol{\Psi}(t+1) \tag{29}$$

where

$$\begin{aligned}\mathbf{Q}(t+1) &= \left[\mathbf{D}(t)^T, \mathbf{D}(t+1)^T\right]\begin{bmatrix}\mathbf{D}(t) \\ \mathbf{D}(t+1)\end{bmatrix} + \eta(t+1)\mathbf{I} \\ &= \mathbf{Q}(t) + \mathbf{D}(t+1)^T\mathbf{D}(t+1) \\ &\quad + (\lambda(t+1) - 1)\eta(t)\mathbf{I}\end{aligned} \tag{30}$$

$$\begin{aligned}\boldsymbol{\Psi}(t+1) &= \left[\mathbf{D}(t)^T, \mathbf{D}(t+1)^T\right]\left[\bar{\mathbf{Y}}(t), \bar{\mathbf{Y}}(t+1)\right]^T \\ &= \boldsymbol{\Psi}(t) + \mathbf{D}(t+1)^T\bar{\mathbf{Y}}(t+1)\end{aligned} \tag{31}$$

where $\mathbf{D}(t+1) = [\mathbf{O}(t+1)\ \mathbf{H}(t+1)]^T$, $\mathbf{O}(t+1) = [\mathbf{o}_1(t+1), \mathbf{o}_2(t+1), \ldots, \mathbf{o}_n(t+1)]$ is the output of IT2FNN layer at time $t+1$, and $\mathbf{H}(t+1) = [\mathbf{h}_1(t+1), \mathbf{h}_2(t+1), \ldots, \mathbf{h}_m(t+1)]$ is the output of enhancement layer at time $t+1$. The output weight $\mathbf{W}(t+1)$ can be rewritten as

$$\begin{aligned}\mathbf{W}(t+1) &= \mathbf{Q}(t+1)^{-1}\Big(\mathbf{Q}(t)\mathbf{Q}(t)^{-1}\mathbf{D}(t)^T\bar{\mathbf{Y}}(t) \\ &\qquad + \mathbf{D}(t+1)^T\bar{\mathbf{Y}}(t+1)\Big) \\ &= \mathbf{Q}(t+1)^{-1}\left(\mathbf{Q}(t)\mathbf{W}(t) + \mathbf{D}(t+1)^T\bar{\mathbf{Y}}(t+1)\right) \\ &= \mathbf{Q}(t+1)^{-1}\Big(\left(\mathbf{Q}(t+1) - \mathbf{D}(t+1)^T\mathbf{D}(t+1)\right)\mathbf{W}(t) \\ &\qquad + \mathbf{D}(t+1)^T\bar{\mathbf{Y}}(t+1)\Big) \\ &= \mathbf{W}(t) + \mathbf{Q}(t+1)^{-1}\mathbf{D}(t+1)^T \\ &\quad \times \left(\bar{\mathbf{Y}}(t+1) - \mathbf{D}(t+1)\mathbf{W}(t)\right)\end{aligned} \tag{32}$$

where

$$\begin{aligned}\mathbf{Q}(t+1)^{-1} &= \Big(\mathbf{Q}(t) + \mathbf{D}(t+1)^T\mathbf{D}(t+1) + (\lambda(t+1) - 1) \\ &\qquad \times \eta(t)\mathbf{D}(t+1)\mathbf{D}(t+1)^{-1}\Big)^{-1} \\ &= \mathbf{Q}(t)^{-1} - \mathbf{Q}(t)^{-1}\Big(\mathbf{D}(t+1)^T + (\lambda(t+1) - 1) \\ &\qquad \times \eta(t)\mathbf{D}(t+1)^{-1}\Big) \\ &\quad \times \Big(\mathbf{I} + \mathbf{D}(t+1)\mathbf{Q}(t)^{-1} \\ &\qquad \times \Big(\mathbf{D}(t+1)^T + (\lambda(t+1) - 1) \\ &\qquad \times \eta(t)\mathbf{D}(t+1)^{-1}\Big)\Big)^{-1}\mathbf{D}(t+1)\mathbf{Q}(t)^{-1}.\end{aligned} \tag{33}$$

Then, it will be

$$\begin{aligned}\mathbf{W}(t+1) &= \mathbf{W}(t) + \boldsymbol{\Theta}(t+1)\mathbf{D}(t+1)^T \\ &\quad \times \left(\bar{\mathbf{Y}}(t+1) - \mathbf{D}(t+1)\mathbf{W}(t)\right)\end{aligned} \tag{34}$$

TABLE I
MAIN PROCEDURE OF THE FPL ALGORITHM

For a nonlinear system, create an initial T2F-BLS. The number of samples is T.
while(t=1 to T)
for sample $\mathbf{X}(t)$
  for i=1:n
    Random the uncertain mean $u_{qsi}(t)$, variance $\sigma_{qsi}(t)$ and interval weight $w_{qki}(t)$;
    Calculate the output of membership layer $\mu_{qsi}(t)$; %Eq. (21)
    Calculate the output of rule layer $\mathbf{f}_{qi}(t)$; %Eqs. (18)-(20)
    Calculate the output of type-reduction layer $[\underline{o}_{ki}(t), \bar{o}_{ki}(t)]$; %Eqs. (16)-(17)
    Calculate the output of a IT2FNN $o_{ki}(t)$; %Eq. (15)
    Calculate the output of IT2FNNs $\mathbf{o}_i(t)$; %Eq. (14)
  end
  Set the output of IT2FNN layer $\mathbf{O}(t)$; %Eq. (13)
  for j=1:m
    Random $\mathbf{w}_{hj}(t)$ and $\boldsymbol{\beta}_{hj}(t)$;
    Calculate the output of the jth group neurons $\mathbf{h}_j(t)$; %Eq. (23)
  end
  Set the output of enhancement layer $\mathbf{H}(t)$; %Eq. (22)
  Update the matrix $\boldsymbol{\Theta}(t+1)$; %Eq. (36)
  Update the output weight $\mathbf{W}(t+1)$; %Eq. (35)
end

where

$$\begin{aligned}\boldsymbol{\Theta}(t+1) = \boldsymbol{\Theta}(t) - \boldsymbol{\Theta}(t)\Big(\mathbf{D}(t+1)^T + (\lambda(t+1)-1) \\ \times \eta(t)\mathbf{D}(t+1)^{-1}\Big) \\ \times \Big(\mathbf{I} + D(t+1)\boldsymbol{\Theta}(t)\Big(\mathbf{D}(t+1)^T + (\lambda(t+1)-1) \\ \times \eta(t)\mathbf{D}(t+1)^{-1}\Big)\Big)^{-1} \\ \mathbf{D}(t+1)\boldsymbol{\Theta}(t) \end{aligned} \tag{35}$$

where $\boldsymbol{\Theta}(t+1) = \mathbf{Q}(t+1)^{-1}$.

To show the process of the FPL algorithm clearly, the main procedure is summarized in Table I.

Remark 2: In fact, the FPL algorithm with the adaptive learning rate can speed up the convergence and enhance the learning performance of T2F-BLS. It may be a burden to compute the maximum and minimum eigenvalues of matrix $\mathrm{D}(t)^T\mathrm{D}(t)$ for adjusting the learning rate $\lambda(t)$. However, with a learning rate embedded in this learning algorithm, the convergence rate can be accelerated and the performance of T2F-BLS can be improved.

Remark 3: The computational complexity of T2F-BLS can be easily deduced based on the structure design and FPL algorithm. Therefore, the time complexity of T2F-BLS is

$$O\left(PS\sum_{i=1}^{n}K_i + P\sum_{i=1}^{n}K_i\sum_{j=1}^{m}L_j + \left(\sum_{i=1}^{n}K_i + \sum_{j=1}^{m}L_j\right)^3\right). \tag{36}$$

C. Convergence Discussion

The convergence analysis of T2F-BLS is an important issue to provide successful applications. In this section, the convergence of T2F-BLS is discussed in detail.

The nonlinear continuous-time form of the system considered in this article is defined by

$$\dot{\mathbf{Y}}(t) = -\mathbf{Y}(t) + \mathbf{G}(\mathbf{Y}(t), \mathbf{X}(t)), \mathbf{Y}(t_0) = \mathbf{Y}_0 \tag{37}$$

$$\dot{\bar{\mathbf{Y}}}(t) = -\bar{\mathbf{Y}}(t) + \bar{\mathbf{G}}\big(\bar{\mathbf{Y}}(t), \mathbf{X}(t)\big), \bar{\mathbf{Y}}(t_0) = \bar{\mathbf{Y}}_0 \tag{38}$$

where $\mathbf{G}(t)$ and $\bar{\mathbf{G}}(t)$ are different unknown nonlinear functions. To present the convergence of T2F-BLS clearly, the approximation error $\mathbf{E}(t)$ of T2F-BLS is

$$\mathbf{E}(t) = \mathbf{Y}(t) - \bar{\mathbf{Y}}(t) \tag{39}$$

where $\mathbf{E}(t) = [E_1(t), E_2(t), \ldots, E_C(t)]$. The approximation error dynamic is

$$\begin{aligned}\dot{\mathbf{E}}(t) &= \dot{\mathbf{Y}}(t) - \dot{\bar{\mathbf{Y}}}(t) \\ &= -\mathbf{Y}(t) + \mathbf{G}(t) + \bar{\mathbf{Y}}(t) - \bar{\mathbf{G}}(t) \\ &= -\mathbf{E}(t) + \mathbf{G}(t) - \bar{\mathbf{G}}(t)\end{aligned} \tag{40}$$

where $\mathbf{E}(t_0) = \mathbf{E}_0$.

Assumption 1 (A1): The training samples are the bounded sequences of independent identically distributed random vectors. *(A2)* : $\mathbf{G}(t)$ and $\bar{\mathbf{G}}(t)$ are bounded continuous functions.

Lemma 1: If assumption A2 is valid, then $||\mathbf{G}(t) - \bar{\mathbf{G}}(t)|| \leq \varepsilon$ ($\varepsilon > 0$ is a positive value).

Proof: Based on assumption A2, $\mathbf{G}(t)$ and $\bar{\mathbf{G}}(t)$ are defined as bounded continuous functions. Due to $\mathbf{O}(t)$ and $\mathbf{H}(t)$ are bounded by construction, the output weights $\mathbf{W}_f(t)$ and $\mathbf{W}_e(t)$ must be bounded to satisfy $||\mathbf{G}(t) - \bar{\mathbf{G}}(t)|| \leq \varepsilon$. ■

Theorem 1: Given the approximation error dynamic of T2F-BLS defined by (40), under the condition that Assumption 1 is satisfied, if $||\mathbf{E}(1)|| = \alpha$ ($\alpha > 0$ is a given positive value), then $||\mathbf{E}(t)|| \leq \alpha$, that is, $\mathbf{E}(t)$ is uniformly ultimately bounded (UUB).

Proof: The Lyapunov function is considered as

$$V(t) = \big(1/2\big)\mathbf{E}(t)^2. \tag{41}$$

According to (40) and (41), the dynamic equation of $V(t)$ will be

$$\begin{aligned}\dot{V}(t) &= \mathbf{E}(t)^T\dot{\mathbf{E}}(t) \\ &= \mathbf{E}(t)^T\big(-\mathbf{E}(t) + \big(\mathbf{G}(t) - \bar{\mathbf{G}}(t)\big)\big) \\ &\leq -\|\mathbf{E}(t)\|^2 + \|\mathbf{E}(t)\|\varepsilon \\ &= -\|\mathbf{E}(t)\|(\|\mathbf{E}(t)\| - \varepsilon).\end{aligned} \tag{42}$$

To prove $\mathbf{E}(t)$ is UUB, the following conditions should be carefully investigated.

1) If $||\mathbf{E}(t)|| > \varepsilon$, $\dot{V}(t) < 0$, and then $||\mathbf{E}(t)|| < \alpha$.
2) If $||\mathbf{E}(t)|| = \varepsilon$, $\dot{V}(t) = 0$, and then $||\mathbf{E}(t)|| = \alpha$.
3) If $||\mathbf{E}(t)|| < \varepsilon$, $\dot{V}(t) > 0$, the solution may reach $||\mathbf{E}(t)|| = \varepsilon$ or $||\mathbf{E}(t)|| > \varepsilon$ at some time. However, when $||\mathbf{E}(t)|| = \varepsilon$ or $||\mathbf{E}(t)|| > \varepsilon$, $\dot{V}(t)$ will be nonpositive, and thus $||\mathbf{E}(t)|| \leq \alpha$. ■

Therefore, the approximation error $\mathbf{E}(t)$ is UUB.

Under the same conditions as in Theorem 1, the modeling error $\mathbf{e}(t)$ is defined as

$$\mathbf{e}(t) = \bar{\mathbf{Y}}(t) - \mathbf{D}(t)\mathbf{W}(t-1) \tag{43}$$

which is the predicted error when estimating the signal $\bar{\mathbf{Y}}(t)$ in the next step using the modeling parameter $\mathbf{D}(t)\mathbf{W}(t-1)$,

$\mathbf{e}(t) = [e_1(t), e_2(t), \ldots, e_C(t)]$. Then, based on (37) and (38), the modeling error dynamic is

$$\begin{aligned}\dot{\mathbf{e}}(t) &= \dot{\bar{\mathbf{Y}}}(t) - \dot{\mathbf{Y}}_m(t)\\ &= -\bar{\mathbf{Y}}(t) + \bar{\mathbf{G}}(t) + \mathbf{Y}_m(t) - \mathbf{G}_m(t)\\ &= -\big(\bar{\mathbf{Y}}(t) - \mathbf{Y}_m(t)\big) + \bar{\mathbf{G}}(t) - \mathbf{G}_m(t)\\ &= -\mathbf{e}(t) + \bar{\mathbf{G}}(t) - \mathbf{G}_m(t)\end{aligned} \tag{44}$$

where $\mathbf{G}(t) = \mathbf{D}(t)\mathbf{W}(t-1)$ and $\mathbf{e}(t_0) = \mathbf{e}_0$.

Assumption 2: $\mathbf{G}_m(t)$ is a bounded continuous function, and $||\bar{\mathbf{G}}(t) - \mathbf{G}_m(t)|| \le \tau(\tau > 0$ is a positive value) is satisfied.

Theorem 2: The modeling error dynamic of T2F-BLS is defined by (44), where Assumption 2 is satisfied. If $||\mathbf{e}(1)|| = \delta(\delta > 0$ is a given positive value), then $||\mathbf{e}(t)|| \le \delta$, that is, $\mathbf{e}(t)$ is UUB.

Proof: The Lyapunov function of $\mathbf{e}(t)$ is defined as

$$V_e(t) = \big(1/2\big)\mathbf{e}(t)^2. \tag{45}$$

Based on (44) and (45), the dynamic equation of $V_e(t)$ is

$$\begin{aligned}\dot{\mathbf{V}}_e(t) &= \mathbf{e}(t)^T\dot{\mathbf{e}}(t)\\ &= \mathbf{e}(t)^T\big(-\mathbf{e}(t) + \big(\bar{\mathbf{G}}(t) - \mathbf{G}_m(t)\big)\big)\\ &\le -\|\mathbf{e}(t)\|^2 + \|\mathbf{e}(t)\|\tau\\ &= -\|\mathbf{e}(t)\|(\|\mathbf{e}(t)\| - \tau).\end{aligned} \tag{46}$$

To prove $\mathbf{e}(t)$ is UUB, the following conditions should be comprehensively considered.

1) If $||\mathbf{e}(t)|| > \tau, \dot{V}_e(t) < 0$, and then $||\mathbf{e}(t)|| < \delta$.
2) If $||\mathbf{e}(t)|| = \tau, \dot{V}_e(t) = 0$, and then $||\mathbf{e}(t)|| = \delta$.
3) If $||\mathbf{e}(t)|| < \tau, \dot{V}_e(t) > 0$, the solution may reach $||\mathbf{e}(t)|| = \tau$ or $||\mathbf{e}(t)|| > \tau$ at some time. However, when $||\mathbf{e}(t)|| = \tau$ or $||\mathbf{e}(t)|| > \tau, \dot{V}_e(t)$ will be nonpositive, and thus $||\mathbf{e}(t)|| \le \delta$. ■

Therefore, the modeling error $\mathbf{e}(t)$ is UUB.

Theorem 3 (Convergence of T2F-BLS With Fixed Learning Rate): Let the proposed T2F-BLS be trained using the updating rules as (35) and (36) and $\lambda(t) = 1$, then the convergence of T2F-BLS can be guaranteed as

$$\lim_{t\to+\infty}|\mathbf{E}(t)| = \mathbf{0}. \tag{47}$$

Proof: Based on (35) and (36), the approximation error $\mathbf{E}(t)$ of T2F-BLS with fixed learning rate is

$$\begin{aligned}\|\mathbf{E}(t)\| &= \left\|\big(\bar{\mathbf{Y}}(t) - \mathbf{D}(t)\mathbf{W}(t-1)\big)\big(\mathbf{I} - \mathbf{D}(t)\boldsymbol{\Theta}(t)(\mathbf{D}(t))^T\big)\right\|\\ &= \left\|\bar{\mathbf{Y}}(t) - \mathbf{D}(t)\mathbf{W}(t-1)\right\|\\ &\quad \left\|\mathbf{I} - \mathbf{D}(t)\big(\boldsymbol{\Theta}(t-1) - \boldsymbol{\Theta}(t-1)(\mathbf{D}(t))^T\right.\\ &\qquad \times \big(\mathbf{I} + \mathbf{D}(t)\boldsymbol{\Theta}(t-1)(\mathbf{D}(t))^T\big)^{-1}\\ &\qquad \left.\times\ \mathbf{D}(t)\Theta(t-1)\big)(\mathbf{D}(t))^T\right\|\\ &= \left\|\frac{\mathbf{e}(t)}{\mathbf{I} + \mathbf{D}(t)\boldsymbol{\Theta}(t-1)(\mathbf{D}(t))^T}\right\|\\ &< \left\|\frac{\mathbf{I}}{\mathbf{I} + \mathbf{D}(t)\boldsymbol{\Theta}(t-1)(\mathbf{D}(t))^T}\right\|\delta.\end{aligned} \tag{48}$$

If $\|\mathbf{I}+\mathbf{D}(t)\boldsymbol{\Theta}(t-1)\ (\mathbf{D}(t))^T\|$ is finite and $\mathbf{D}(t)\boldsymbol{\Theta}(t-1)(\mathbf{D}(t))^T$ is not equal to $-\mathbf{I}$ over the entire time period, and the conditions in (35) and (36) are always met during the training process, it will be

$$1 \le \left\|\mathbf{I} + \mathbf{D}(t)\boldsymbol{\Theta}(t-1)(\mathbf{D}(t))^T\right\| \le z \tag{49}$$

where z is a positive constant. As δ is an arbitrary positive small value, $\|\mathbf{I}/(\mathbf{I}+\mathbf{D}(t)\boldsymbol{\Theta}\ (t-1)(\mathbf{D}(t))^T)\|\delta$ is also an arbitrary positive small value. Thus, it is easy to verify that the convergence of T2F-BLS can be guaranteed with $\mathbf{E}(t)\to 0$ as $t\to 0$. Therefore, the proof of Theorem 3 is completed. ■

Theorem 4 (Convergence of T2F-BLS With Adaptive Learning Rate): Let the conditions of Theorem 3 hold and the learning rate $\eta(t)$ can be defined as (27) and (28). Then, the convergence of T2F-BLS can be guaranteed.

Proof: Based on (35) and (36), the approximation error $\mathbf{E}_a(t)$ of T2F-BLS with the adaptive learning rate is

$$\begin{aligned}\|\mathbf{E}_a(t)\| &= \left\|\big(\bar{\mathbf{Y}}(t) - \mathbf{D}(t)\mathbf{W}(t-1)\big)\Big(\mathbf{I} - \mathbf{D}(t)\boldsymbol{\Theta}(t)(\mathbf{D}(t))^T\Big)\right\|\\ &= \left\|\bar{\mathbf{Y}}(t) - \mathbf{D}(t)\mathbf{W}(t-1)\right\|\\ &\quad \times \left\|\mathbf{I} - \mathbf{D}(t)\ (\boldsymbol{\Theta}(t-1) - \boldsymbol{\Theta}(t-1)\right.\\ &\qquad \times \Big((\mathbf{D}(t))^T + (\lambda(t)-1)\eta(t-1)\mathbf{D}(t)^{-1}\Big)\\ &\qquad \times\ (\mathbf{I} + \mathbf{D}(t)\boldsymbol{\Theta}(t-1)\\ &\qquad \times\ \Big((\mathbf{D}(t))^T + (\lambda(t)-1)\eta(t-1)\mathbf{D}(t)^{-1}\Big)\Big)^{-1}\\ &\qquad \left.\times\ \mathbf{D}(t)\boldsymbol{\Theta}(t-1))(\mathbf{D}(t))^T\right\|\\ &= \frac{\|e(t)\|\left\|\mathbf{I} + \mathbf{D}(t)\boldsymbol{\Theta}(t-1)(\lambda(t)-1)\eta(t-1)\mathbf{D}(t)^{-1}\right\|}{\left\|\mathbf{I} + \mathbf{D}(t)\boldsymbol{\Theta}(t-1)\big((\mathbf{D}(t))^T + (\lambda(t)-1)\eta(t-1)\mathbf{D}(t)^{-1}\big)\right\|}.\end{aligned} \tag{50}$$

Then, based on (48) and (50), the error between $\mathbf{E}_a(t)$ and $\mathbf{E}(t)$ is calculated as

$$\begin{aligned}\|\mathbf{E}_a(t) - \mathbf{E}(t)\| &= \left\|\frac{\mathbf{e}(t)(\mathbf{I} + \boldsymbol{\Xi}(t))}{\mathbf{I} + \boldsymbol{\Lambda}(t) + \boldsymbol{\Xi}(t)} - \frac{\mathbf{e}(t)}{\mathbf{I} + \boldsymbol{\Lambda}(t)}\right\|\\ &= \|\mathbf{e}(t)\|\left\|\frac{\mathbf{D}(t)\boldsymbol{\Theta}(t-1)\boldsymbol{\Xi}(t)}{(\mathbf{I} + \boldsymbol{\Lambda}(t) + \boldsymbol{\Xi}(t))(\mathbf{I} + \boldsymbol{\Lambda}(t))}\right\|\end{aligned} \tag{51}$$

where

$$\boldsymbol{\Lambda}(t) = \mathbf{D}(t)\boldsymbol{\Theta}(t-1)(\mathbf{D}(t))^T \tag{52}$$

$$\boldsymbol{\Xi}(t) = \mathbf{D}(t)\boldsymbol{\Theta}(t-1)(\lambda(t)-1)\eta(t-1)\mathbf{D}(t)^{-1}. \tag{53}$$

According to the learning rate $\eta(t)$ of the weight optimizing strategy defined by (27) and (28), and $0 < \eta(t) < 1$, there exits

$$1 - \frac{\tau^{\min}(t-1)(\tau^{\max}(t-1)+1)}{\tau^{\max}(t-1)} < \eta(t-1). \tag{54}$$

Then, it can obtain $\lambda(t) < 1$. Based on (52)–(54), it yields $||\boldsymbol{\Xi}(t)|| < 0$, then (51) will be

$$\|\mathbf{E}_a(t) - \mathbf{E}(t)\| \le \|\mathbf{e}(t)\|\left\|\frac{\mathbf{D}(t)\boldsymbol{\Theta}(t-1)\boldsymbol{\Xi}(t)}{(\mathbf{I} + \boldsymbol{\Lambda}(t) + \boldsymbol{\Xi}(t))^2}\right\| < 0. \tag{55}$$

From the results in Theorem 3, it can be observed that $\mathbf{E}_a(t)\to 0$ as $t\to 0$. Then, the convergence of T2F-BLS with the adaptive learning rate can be guaranteed. By now, the proof of Theorem 4 is completed. ■

Remark 4: Based on Theorems 1 and 2, the approximation error and the modeling error of T2F-BLS are UUB. Meanwhile, the convergence of T2F-BLS with the fixed learning rate and adaptive learning rate can also be proved. This property of T2F-BLS can ensure its applications.

IV. Experimental Studies

In this section, the proposed T2F-BLS is applied to two examples: 1) the prediction of classical multiple-input multiple-output (MIMO) system and 2) the prediction of wastewater treatment process (WWTP). The results are compared with some other existing methods.

Moreover, the parameter setting plays an important role in ensuring the performance of T2F-BLS. The total numbers of IT2FNN subsystems n and fuzzy rules K for input variables are chosen from $\{1, 2, \ldots, 10\}$ and $\{2, 3, \ldots, 20\}$, respectively, while the number of group enhancement neurons m and the number of neurons L in a group enhancement neuron locate in $\{2, 3, \ldots, 20\}$ and $\{2, 3, \ldots, 100\}$, respectively. In order to ensure a fair comparison, parameters that can achieve the best testing accuracy are generated through a grid search for T2F-BLS and other comparison methods. Then, the prediction abilities of all the methods are tested in a MIMO system and WWTP. All the experiments are repeated 30 times on every dataset with different conditions. The simulations are programmed with MATLAB version 2016 and run on a PC with a clock speed of 2.6 GHz and 8-GB RAM, under a Microsoft Windows 8.0 64-bit OS.

The performance of different methods is evaluated by using the root mean square error (RMSE) and the mean absolute percentage error (MAPE)

$$\text{RMSE}(t) = \sqrt{\frac{1}{T}\sum_{t=1}^{T}\left(\mathbf{Y}(t) - \bar{\mathbf{Y}}(t)\right)^T\left(\mathbf{Y}(t) - \bar{\mathbf{Y}}(t)\right)} \quad (56)$$

$$\text{MAPE}(t) = \frac{1}{T}\sum_{t=1}^{T}\frac{\left\|\mathbf{Y}(t) - \bar{\mathbf{Y}}(t)\right\|}{\left\|\bar{\mathbf{Y}}(t)\right\|} \times 100\%. \quad (57)$$

The experimental results of RMSE and MAPE are the average values in the different conditions.

A. Prediction of Nonlinear Dynamic System

To assess the performance of T2F-BLS for modeling the nonlinear dynamic system, a popular system is given by [16]

$$y(t) = \frac{y(t-1)y(t-2)(y(t-1)+2.5)}{1+y(t-1)^2+y(t-2)^2} + x(t-1) \quad (58)$$

where $x(t)$ is the input signal, $x(t-1)$, $y(t-1)$, and $y(t-2)$ are the input variables of the system, and $y(t)$ is the output variables of system. Meanwhile, the training samples are selected from $t = 1$ to $t = 5000$, where $x(t)$ is produced from the range of $[-2, 2]$ with some noises uniformly distributing in $[-0.2, 0.2]$. The testing samples are chosen from $t = 5001$ to $t = 5200$, where $x(t) = \sin(2\pi t/25)$. Moreover, in this experiment, the number of IT2FNN subsystems n and fuzzy rules K are 4 and 8. The number of group enhancement neurons m and neurons in a group enhancement neuron L are 10 and 60.

TABLE II
Comparison Results for the Nonlinear Dynamic System

Methods	RMSE	MAPE	Time
T2F-BLS (adaptive)	**0.0162**	**0.0061**	**2.497**
T2F-BLS (fixed)	**0.0193**	**0.0072**	**3.024**
BLS [1]	0.0265	0.0102	0.074
FBLS [16]	0.0246	0.0094	1.857
RR-BLS [9]	0.0223	0.0088	3.879
RM-BLS [11]	0.0217	0.0085	4.415
WT1FNN [15]	0.2196	0.0825	26.849
IT2FNN [22]	0.1268	0.0568	31.127

To demonstrate the performance of T2F-BLS, the results of T2F-BLS are compared with some other methods: BLS [1], FBLS [16], RR-BLS [9], RM-BLS [11], WT1FNN [15], and IT2FNN [22]. In particular, T2F-BLS (adaptive) is the proposed method with the adaptive learning rate and T2F-BLS (fixed) is the proposed method with the fixed learning rate. The training and testing samples are used for these methods. The simulation results, including the testing RMSE, testing MAPE, and testing time, are given in Fig. 2 and Table II.

Comparison of Testing RMSE: It can be seen that the proposed T2F-BLS can achieve the least values of testing RMSE among all methods in Fig. 2(a). Meanwhile, the results in Table II illustrate that the proposed T2F-BLS with adaptive learning rate can own better testing RMSE (0.0162) than other methods.

Comparison of Testing MAPE: The results in Fig. 2(b) show that the testing MAPE of T2F-BLS is better than other methods. Moreover, the results in Table II demonstrate that the testing MAPE (0.0061) of T2F-BLS with the adaptive learning rate is less than other methods.

Comparison of Testing Time: As shown in Fig. 2(c), the proposed T2F-BLS with adaptive learning rate is able to cost less testing time than RR-BLS, RM-BLS, WT1FNN, and IT2FNN. Furthermore, the testing time of T2F-BLS with the adaptive learning rate (2.497 s) is better than some other methods in Table II.

In this comparative analysis, the experimental results have verified that the proposed T2F-BLS with T2-FS can achieve the best performance in terms of testing RMSE and testing MAPE. The similar phenomenon can also be found in the comparison results of WT1FNN and IT2FNN. Therefore, it can be concluded that the robust performance of T2F-BLS is attributed to the superiority of its structural design. Moreover, as pointed out in the results of testing time, compared with RR-BLS and RM-BLS, it can be seen that the proposed T2F-BLS costs less time, which confirms the importance of the FPL algorithm. Meanwhile, due to the existence of an adaptive learning rate, the testing time of T2F-BLS (adaptive) is less than the T2F-BLS (fixed). However, with T2-FS embedded, the testing time of T2F-BLS is a little more than that of BLS and FBLS, and the testing time of IT2FNN is a little

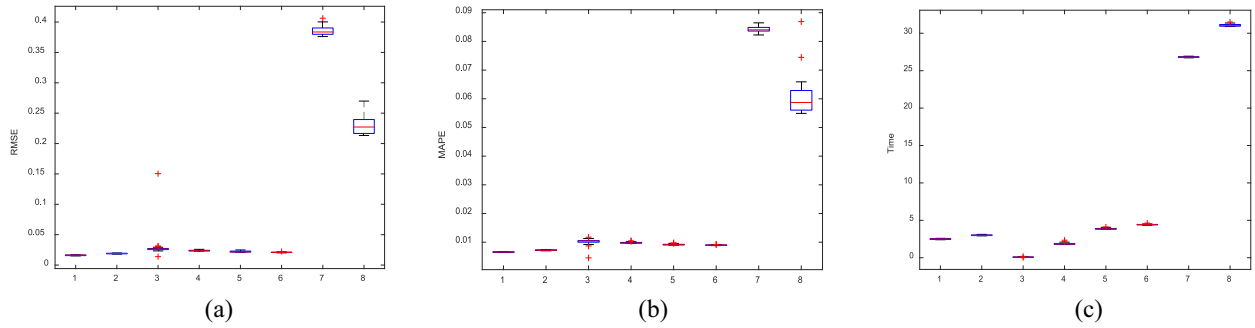

Fig. 2. Box-plots of different methods for nonlinear dynamic system. (1, 2, 3, 4, 5, 6, 7, and 8 in the horizontal axis stand for T2F-BLS (adaptive), T2F-BLS (fixed), BLS, FBLS, RR-BLS, RM-BLS, WT1FNN, and IT2FNN). (a) RMSE of different methods. (b) MAPE of different methods. (c) Time of different methods.

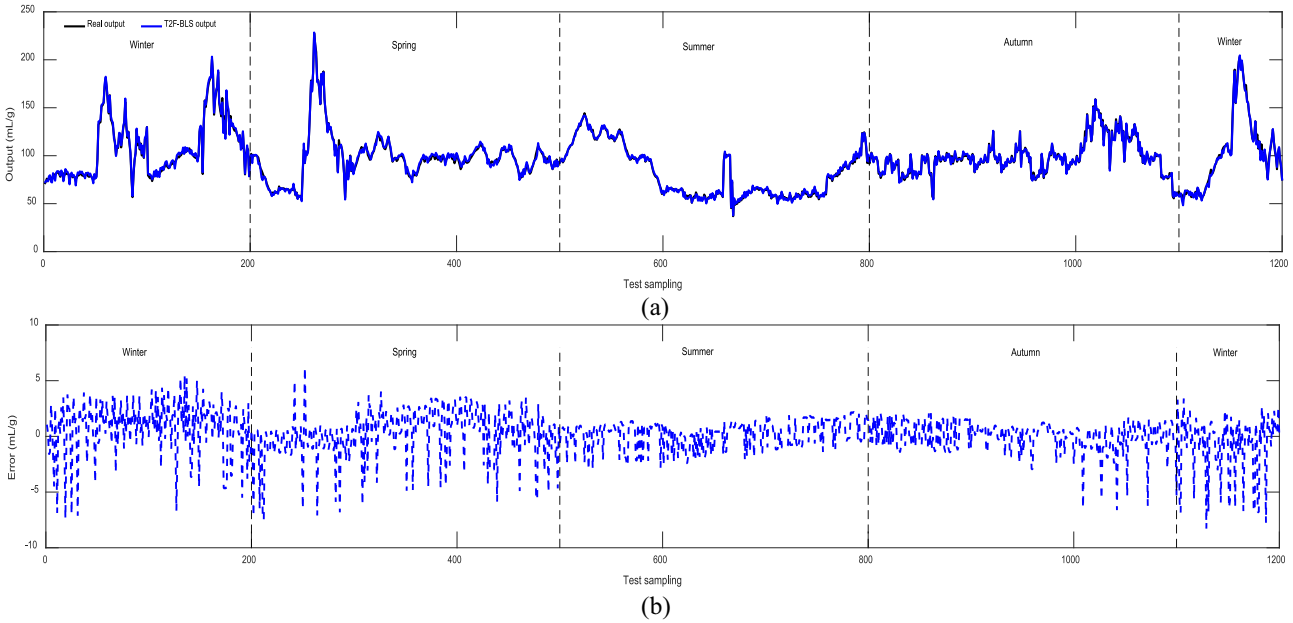

Fig. 3. (a) Prediction results of T2F-BLS. (b) Prediction error results of T2F-BLS.

more than that of WT1FNN. Considering its good prediction accuracy, the balance between efficiency and effectiveness can still be maintained well by the proposed T2F-BLS. All of the results illustrate that the BLS methods are proved to be better than WT1FNN and IT2FNN in terms of testing RMSE, testing MAPE, and testing time. The proposed T2F-BLS can approximate the nonlinear dynamic system with better robust performance and less computational time than other methods.

B. Prediction of Wastewater Treatment Process

Due to the physical and biochemical actions, WWTP is always run in the nonsteady-state condition. It is difficult to obtain an accurate model to satisfy the complex and uncertain characters of WWTP [35]. The measurement techniques are often scarce. Thus, the parameter identification of WWTP still appears as an open problem [36]. To address this problem, the proposed T2F-BLS is used to predict the parameter of WWTP. To test the performance of T2F-BLS, the proposed T2F-BLS is used to predict the sludge bulking in the anaerobic/anoxic/oxic process. The input–output datasets are obtained from real WWTPs (Beijing, China) over the year 2018. In each season, 500 data samples are collected in the training dataset, and 300 data samples are chosen in the testing dataset.

In this example, the proposed T2F-BLS is used to predict the sludge bulking with the related input variables-dissolved oxygen concentration (DO(t)), total nutrients (TN(t)), organic load rate (F/M(t)), potential of hydrogen (pH(t)), temperature (T(t)), and the output variable SVI(t). SVI(t) is used as an index to quantify sludge bulking [37]. Moreover, the number of IT2FNN subsystems n and fuzzy rules K are 6 and 12. The number of group enhancement neurons m and neurons in a group enhancement neuron L are 12 and 80. Meanwhile, the measurable disturbance and noise have been considered in the experiment.

The prediction results and the prediction error results of T2F-BLS are displayed in Fig. 3(a) and (b), respectively. Due to the frequent occurrence of sludge bulking in spring and winter, the noise will influence the performance of T2F-BLS. Then, the prediction error in spring and winter is larger than that in summer and autumn. The proposed T2F-BLS,

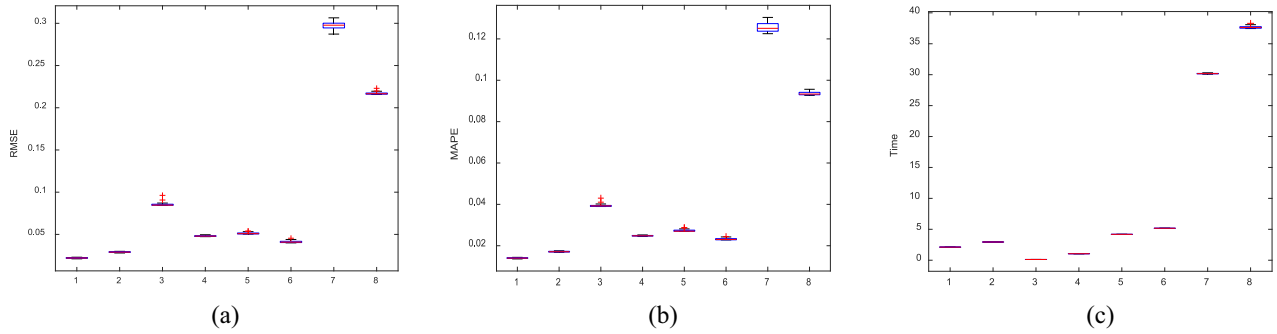

Fig. 4. Box-plots of different methods in spring. (1, 2, 3, 4, 5, 6, 7, and 8 in the horizontal axis stand for T2F-BLS (adaptive), T2F-BLS (fixed), BLS, FBLS, RR-BLS, RM-BLS, WT1FNN, and IT2FNN). (a) RMSE of different methods. (b) MAPE of different methods. (c) Time of different methods.

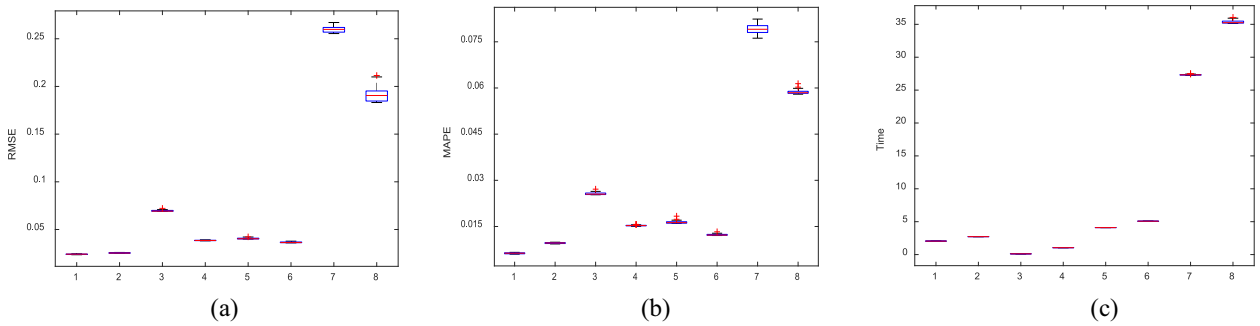

Fig. 5. Box-plots of different methods in summer. (1, 2, 3, 4, 5, 6, 7, and 8 in the horizontal axis stand for T2F-BLS (adaptive), T2F-BLS (fixed), BLS, FBLS, RR-BLS, RM-BLS, WT1FNN, and IT2FNN). (a) RMSE of different methods. (b) MAPE of different methods. (c) Time of different methods.

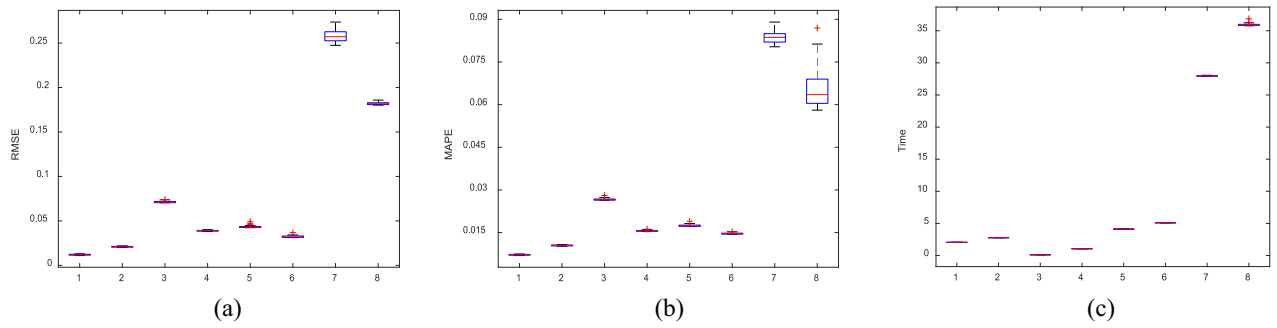

Fig. 6. Box plots of different methods in autumn. (1, 2, 3, 4, 5, 6, 7, and 8 in the horizontal axis stand for T2F-BLS (adaptive), T2F-BLS (fixed), BLS, FBLS, RR-BLS, RM-BLS, WT1FNN, and IT2FNN). (a) RMSE of different methods. (b) MAPE of different methods. (c) Time of different methods.

based on the structure design and learning algorithm, is able to provide accurate and reliable prediction results in this experiment.

To evaluate the performance of T2F-BLS, the results of T2F-BLS are compared with other methods: BLS [1], FBLS [16], RR-BLS [9], RM-BLS [11], WT1FNN [15], and IT2FNN [22]. The results of testing RMSE, testing MAPE, and testing time are detailed in Figs. 4–7 and Table III. Meanwhile, all methods are run 50 times and the results in Table III are the average of 50 trials.

Comparison of Testing RMSE: Figs. 4–7(a) illustrate that the proposed T2F-BLS can obtain better performance of testing RMSE than other methods. Meanwhile, the results in Table III show that the proposed T2F-BLS with the adaptive learning algorithm can own the least values of testing RMSE (0.0422, 0.0275, 0.0311, and 0.0582) than other methods.

Comparison of Testing MAPE: The results in Figs. 4–7(b) demonstrate that the testing MAPE of T2F-BLS is better than the other six methods. Moreover, the testing MAPE of T2F-BLS with adaptive learning rate (0.0141, 0.0098, 0.0105, and 0.0185) is less than other methods in Table III.

Comparison of Testing Time: Figs. 4–7(c) show that the testing time of T2F-BLS is less than some other methods. Meanwhile, the results in Table III illustrate that the proposed T2F-BLS with adaptive learning rate can own less values of testing time (2.121, 2.049, 2.055, and 2.141 s) than other methods (except for BLS and FBLS).

It is worth noting that due to the introduction of T2-FS, the proposed T2F-BLS can achieve better prediction performance than other BLSs, WT1FNN, and IT2FNN in terms of testing RMSE and testing MAPE. The similar conclusion can also be summarized from the results of WT1FNN and IT2FNN. It can

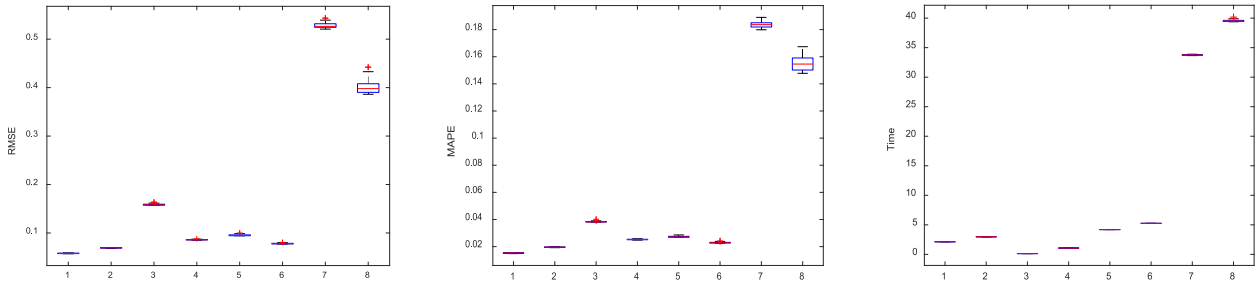

Fig. 7. Box plots of different methods in winter (1, 2, 3, 4, 5, 6, 7, and 8 in the horizontal axis stand for T2F-BLS (adaptive), T2F-BLS (fixed), BLS, FBLS, RR-BLS, RM-BLS, WT1FNN, and IT2FNN). (a) RMSE of different methods. (b) MAPE of different methods. (c) Time of different methods.

TABLE III
COMPARISON RESULTS OF DIFFERENT METHODS

Mehtods	Seasons											
	Spring			Summer			Autumn			Winter		
	RMSE	MAPE	Time	RMSE	MAPE	Time	RMSE	MAPE	Time	RMSE	MAPE	Time
T2F-BLS (adaptive)	**0.0422**	**0.0141**	**2.121**	**0.0275**	**0.0098**	**2.049**	**0.0311**	**0.0105**	**2.055**	**0.0582**	**0.0185**	**2.141**
T2F-BLS (fixed)	**0.0514**	**0.0176**	**2.945**	**0.0327**	**0.0109**	**2.726**	**0.0367**	**0.0124**	**2.775**	**0.0744**	**0.0258**	**2.979**
BLS [1]	0.0887	0.0387	0.122	0.0601	0.0282	0.112	0.0683	0.0301	0.115	0.1284	0.0427	0.134
FBLS [16]	0.0598	0.0217	1.055	0.0403	0.0134	1.048	0.0457	0.0154	1.051	0.0867	0.0282	1.071
RR-BLS [9]	0.0624	0.0228	4.186	0.0427	0.0148	4.102	0.0471	0.0169	4.113	0.0958	0.0318	4.199
RM-BLS [11]	0.0571	0.0203	5.169	0.0382	0.0121	5.075	0.0432	0.0141	5.096	0.0782	0.0251	5.254
WT1FNN [15]	0.3161	0.1251	30.215	0.2631	0.0826	27.364	0.2816	0.0894	28.024	0.5191	0.1822	33.794
IT2FNN [22]	0.2252	0.0886	37.687	0.1874	0.0549	35.357	0.1668	0.0614	35.997	0.3552	0.1571	39.614

be concluded that the IT2FNN structure can improve the robust performance of T2F-BLS. Meanwhile, it is easy to see that the proposed T2F-BLS retains the fast computational nature of BLS since the parameters are also calculated by pseudoinverse. On the contrary, other fuzzy models (WT1FNN and IT2FNN) are usually trained in an iterative manner. Hence, the testing process of T2F-BLS is fast and efficient. The existence of an adaptive learning rate can accelerate the convergence rate and reduce the testing time of T2F-BLS in particular. However, due to the design structure of T2-FS, the proposed T2F-BLS and IT2FNN need more testing time than other methods in the learning process. Although the proposed T2F-BLS is slightly slower than BLS and FBLS, in view of good prediction accuracy, the tradeoff between model accuracy and learning efficiency can still be guaranteed by T2F-BLS. Hence, the results demonstrate that T2F-BLS can obtain better prediction performance for sludge bulking than other methods under different seasons.

C. Statistical Analysis

To show the statistically significant differences among the aforementioned 8 methods over the databases. The databases have different types of variables and their details are presented in Table IV.

The Friedman test with confidence level $\alpha = 0.05$ is used to evaluate the performance of different methods, including prediction accuracy and computational time. The testing results are demonstrated in Table V. It can be seen that

TABLE IV
DETAILS OF DATASETS FOR PREDICTION

Datasets		No. of Samples		No. of Features
		Training	Testing	
Nonlinear System		5000	200	3
Sludge Bulking	Spring	500	300	5
	Summer	500	300	5
	Autumn	500	300	5
	Winter	500	300	5
Membrane Fouling	Spring	500	300	8
	Summer	500	300	8
	Autumn	500	300	8
	Winter	500	300	8

the BLSs can own better performance than WT1FNN and IT2FNN methods from the second to the fourth rows (about prediction accuracy). Meanwhile, as seen from Table V, the proposed T2F-BLS is able to obtain the top rank in the prediction accuracy. The p-value of prediction accuracy is $1.15\times10^{-6}<<0.05$, which reflects that there are significant differences among different methods. Moreover, the last three rows in Table V indicate that the average rankings in computational time of BLSs are more efficient than other methods. The T2F-BLS can achieve better results of time rank than RR-BLS, RM-BLS, WT1FNN, and IT2FNN. Although the computational time of T2F-BLS is slightly slower than BLS and FBLS, the balance between efficiency and effectiveness can still be maintained well because of its good prediction accuracy. The

TABLE V
AVERAGE RANKINGS OF DIFFERENT METHODS IN PREDICTION ACCURACY AND COMPUTATIONAL TIME

Mehtods	Prediction Accuracy		Computational Time	
	Ranks	*p*-value	Ranks	*p*-value
T2F-BLS (adaptive)	1	1.15×10^{-6}	3	3.27×10^{-6}
T2F-BLS (fixed)	2		4.52	
BLS [1]	6		1	
FBLS [16]	5.56		2	
RR-BLS [9]	3.15		4.89	
RM-BLS [11]	4.47		5.24	
WT1FNN [15]	8		7	
IT2FNN [22]	7		8	

p-value is $3.27\times10^{-6}<<0.05$, which illustrates the significant differences in the computational time of different methods.

D. Results Analysis

The above results indicate that the proposed T2F-BLS can deal with the typical benchmark prediction problem and the real-world application under an uncertain environment. Based on the experimental results, the proposed T2F-BLS has the following advantages.

1) *Good Robust Performance:* A group of interval type-2 fuzzy neurons are used to replace the feature neurons of traditional BLS. The structure design of IT2FNN is introduced to improve the representation ability of T2F-BLS to improve the robustness. The results of the benchmark and real experiments demonstrate that the proposed T2F-BLS can own good results of testing RMSE and testing MAPE.
2) *Fast Learning Speed:* An FPL algorithm is developed to update the output weights of the proposed T2F-BLS in the learning process. The adaptive learning rate strategy can reduce the computational time of T2F-BLS. Moreover, the comparison results have illustrated that the proposed T2F-BLS, based on this effective learning algorithm, is able to obtain less testing time than some other methods.

V. CONCLUSION

In this article, a type of T2F-BLS was proposed to improve the robust performance to deal with the uncertainties. In this T2F-BLS, a set of interval type-2 fuzzy neurons was developed to replace the feature neurons of BLS. The structure of IT2FNN can improve the ability of representation to alleviate the effect of disturbance. The experimental results illustrated that the proposed T2F-BLS is able to obtain better robust performance than other BLSs. Meanwhile, the proposed FPL algorithm with an adaptive learning rate can reduce computational time. The results demonstrated that the proposed T2F-BLS is able to obtain less testing time than other existing methods. Therefore, based on the above analysis, it can be concluded that the proposed T2F-BLS can obtain good performance in terms of robustness and computational time under an uncertain environment.

In addition, since the structure size is important for the performance of T2F-BLS, the future study will focus on the self-organizing T2F-BLS to improve its performance for some other problems.

REFERENCES

[1] C. L. P. Chen and Z. Liu, "Broad learning system: An effective and efficient incremental learning system without the need for deep architecture," *IEEE Trans. Neural Netw. Learn. Syst.*, vol. 29, no. 1, pp. 10–24, Jan. 2018.

[2] C. L. P. Chen, Z. Liu, and S. Feng, "Universal approximation capability of broad learning system and its structural variations," *IEEE Trans. Neural Netw. Learn. Syst.*, vol. 30, no. 4, pp. 1191–1204, Apr. 2018.

[3] M. L. Xu, M. Han, C. L. P. Chen, and T. Qiu, "Recurrent broad learning systems for time series prediction," *IEEE Trans. Cybern.*, vol. 50, no. 4, pp. 1405–1417, Apr. 2020.

[4] J. Feng, Y. Yu, S. X. Lu, and Y. Liu, "Domain knowledge-based deep-broad learning framework for fault diagnosis," *IEEE Trans. Ind. Electron.*, vol. 68, no. 4, pp. 3454–3464, Apr. 2021.

[5] H. M. Zhao, J. J. Zheng, W. Deng, and Y. J. Song, "Semi-supervised broad learning system based on manifold regularization and broad network," *IEEE Trans. Circuits Syst. I, Reg. Papers*, vol. 67, no. 3, pp. 983–994, Mar. 2020.

[6] W. K. Yu and C. H. Zhao, "Broad convolutional neural network based industrial process fault diagnosis with incremental learning capability," *IEEE Trans. Ind. Electron.*, vol. 67, no. 6, pp. 5081–5091, Jun. 2020.

[7] H. M. Zhao, J. J. Zheng, J. J. Xu, and W. Deng, "Fault diagnosis method based on principal component analysis and broad learning system," *IEEE Access*, vol. 7, pp. 99263–99272, 2019.

[8] J. C. Fan, X. Wang, X. X. Wang, J. H. Zhao, and X. X. Liu, "Incremental wishart broad learning system for fast PolSAR image classification," *IEEE Geosci. Remote Sens. Lett.*, vol. 16, no. 12, pp. 1854–1858, Dec. 2019.

[9] J. W. Jin and C. L. P. Chen, "Regularized robust broad learning system for uncertain data modeling," *Neurocomputing*, vol. 322, pp. 58–69, Dec. 2018.

[10] F. Chu, T. Liang, C. L. P. Chen, X. S. Wang, and X. P. Ma, "Weighted broad learning system and its application in nonlinear industrial process modeling," *IEEE Trans. Neural Netw. Learn. Syst.*, vol. 31, no. 8, pp. 3017–3031, Aug. 2020.

[11] S. Feng, W. Ren, M. Han, and Y. W. Chen, "Robust manifold broad learning system for large-scale noisy chaotic time series prediction: A perturbation perspective," *Neural Netw.*, vol. 117, pp. 179–190, Sep. 2019.

[12] X. Y. Zhang, S. Q. Wang, J. B. Hoagg, and T. M. Seigler, "The roles of feedback and feedforward as humans learn to control unknown dynamic systems," *IEEE Trans. Cybern.*, vol. 48, no. 2, pp. 543–555, Feb. 2018.

[13] X Wang, Z. Q. Hou, W. S. Yu, Z. Jin, Y. F. Zha, and X. X. Qin, "Online scale adaptive visual tracking based on multilayer convolutional features," *IEEE Trans. Cybern.*, vol. 49, no. 1, pp. 146–158, Jan. 2019.

[14] L. M. Wang, H. B. He, Z. G. Zeng, and C. Hu, "Global stabilization of fuzzy memristor-based reaction–Diffusion neural networks," *IEEE Trans. Cybern.*, vol. 50, no. 11, pp. 4658–4669, Nov. 2020.

[15] J. Zhao and C.-M. Lin, "Wavelet-TSK-Type fuzzy cerebellar model neural network for uncertain nonlinear systems," *IEEE Trans. Fuzzy Syst.*, vol. 27, no. 3, pp. 549–558, Mar. 2019.

[16] S. Feng and C. L. P. Chen, "Fuzzy broad learning system: A novel neuro-fuzzy model for regression and classification," *IEEE Trans. Cybern.*, vol. 50, no. 2, pp. 414–424, Feb. 2020.

[17] H. Guo, B. Sheng, P. Li, and C. L. P. Chen, "Multiview high dynamic range image synthesis using fuzzy broad learning system," *IEEE Trans. Cybern.*, early access, Aug. 30, 2019, doi: 10.1109/TCYB.2019.2934823.

[18] S. Feng and C. L. P. Chen, "Nonlinear system identification using a simplified fuzzy broad learning system: Stability analysis and a comparative study," *Neurocomputing*, vol. 337, pp. 274–286, Apr. 2019.

[19] D. Zhong and F. G. Liu, "RF-OSFBLS: An RFID reader-fault-adaptive localization system based on online sequential fuzzy broad learning system," *Neurocomputing*, vol. 390, pp. 28–39, May 2020.

[20] H. G. Han, L. Zhang, X. L. Wu, and J. F. Qiao, "An efficient second-order algorithm for self-organizing fuzzy neural networks," *IEEE Trans. Cybern.*, vol. 49, no. 1, pp. 14–26, Jan. 2019.

[21] C. Peng, R. W. Lu, O. Kang, and W. Kai, "Batch process fault detection for multi-stage broad learning system," *Neural Netw.*, vol. 129, pp. 298–312, Sep. 2020.
[22] I. Eyoh, R. John, G. De Maere, and E. Kayacan, "Hybrid learning for interval type-2 intuitionistic fuzzy logic systems as applied to identification and prediction problems," *IEEE Trans. Fuzzy Syst.*, vol. 26, no. 5, pp. 2672–2685, Oct. 2018.
[23] C.-M. Lin, T.-L. Le, and T.-T. Huynh, "Self-evolving function-link interval type-2 fuzzy neural network for nonlinear system identification and control," *Neurocomputing*, vol. 275, pp. 2239–2250, Jan. 2018.
[24] H.G. Han, Z. Y. Chen, H. X. Liu and J. F. Qiao, "A self-organizing interval type-2 fuzzy-neural-network for modeling nonlinear systems," *Neurocomputing*, vol. 290, pp. 196–207, May 2018.
[25] Y. Y. Lin, J. Y. Chang, and C. T. Lin, "A TSK-type-based self-evolving compensatory interval type-2 fuzzy neural network (TSCIT2FNN) and its applications," *IEEE Trans. Ind. Electron.*, vol. 61, no. 1, pp. 447–459, Jan. 2014.
[26] P. K. Muhuri, Z. Ashraf, and Q. M. D. Lohani, "Multiobjective reliability redundancy allocation problem with interval type-2 fuzzy uncertainty," *IEEE Trans. Fuzzy Syst.*, vol. 26, no. 3, pp. 1339–1355, Jun. 2018.
[27] T.-L. Le, C.-M. Lin, and T.-T. Huynh, "Self-evolving type-2 fuzzy brain emotional learning control design for chaotic systems using PSO," *Appl. Soft Comput.*, vol. 73, pp. 418–433, Dec. 2018.
[28] H.-G. Han, J.-M. Li, X.-L. Wu, and J.-F. Qiao, "Cooperative strategy for constructing interval type-2 fuzzy neural network," *Neurocomputing*, vol. 365, pp. 249–260, Nov. 2019.
[29] Y. Jarraya, S. Bouaziz, H. Hagras, and A. M. Alimi, "A multi-agent architecture for the design of hierarchical interval type-2 beta fuzzy system," *IEEE Trans. Fuzzy Syst.*, vol. 27, no. 6, pp. 1174–1188, Jun. 2019.
[30] C. F. Liu, L. Feng, S. Guo, H. B. Wang, S. L. Liu, and H. Qiao, "An incrementally cascaded broad learning framework to facial landmark tracking," *Neurocomputing*, vol. 410, pp. 125–137, Oct. 2020.
[31] Q. M. Zhou and X. P. He, "Broad learning model based on enhanced features learning," *IEEE Access*, vol. 7, pp. 42536–42550, Mar. 2019.
[32] Y. Long, Z. Chen, and S. Murphy, "Broad learning based hybrid beamforming for mm-wave MIMO in time-varying environments," *IEEE Commun. Lett.*, vol. 24, no. 2, pp. 358–361, Feb. 2020.
[33] T. Zhao and S. Dian, "State feedback control for interval type-2 fuzzy systems with time-varying delay and unreliable communication links," *IEEE Trans. Fuzzy Syst.*, vol. 26, no. 2, pp. 951–966, Apr. 2018.
[34] Y. H. Shen, W. Pedrycz, and X. M. Wang, "Approximation of fuzzy sets by interval type-2 trapezoidal fuzzy sets," *IEEE Trans. Cybern.*, vol. 50, no. 11, pp. 4722–4734, Nov. 2020.
[35] H. G. Han, Z. Liu, Y. Hou, and J. F. Qiao, "Data-driven multiobjective predictive control for wastewater treatment process," *IEEE Trans. Ind. Informat.*, vol. 16, no. 4, pp. 2767–2775, Apr. 2020.
[36] H.-G. Han, Z. Liu, Y.-N. Guo, and J.-F. Qiao, "An intelligent detection method for bulking sludge of wastewater treatment process," *J. Process Control*, vol. 68, pp. 118–128, Aug. 2018.
[37] Z. D. Hao, B. Q. Yang, and D. Jahng, "Spent coffee ground as a new bulking agent for accelerated biodrying of dewatered sludge," *Water Res.*, vol. 138, pp. 250–263, Jul. 2018.

Honggui Han (Senior Member, IEEE) received the B.S. degree in automatic control from Civil Aviation University of China, Tianjin, China, in 2005, the M.E. and Ph.D. degrees in control theory and control engineering from the Beijing University of Technology, Beijing, China, in 2007 and 2011, respectively.

He has been with the Beijing University of Technology since 2011, where he is currently a Professor. His current research interests include neural networks, fuzzy systems, intelligent systems, modeling and control in process systems, and civil and environmental engineering.

Prof. Han is currently a Reviewer of IEEE TRANSACTIONS ON FUZZY SYSTEMS, IEEE TRANSACTIONS ON NEURAL NETWORKS AND LEARNING SYSTEMS, IEEE TRANSACTIONS ON CYBERNETICS, and IEEE TRANSACTIONS ON CONTROL SYSTEMS TECHNOLOGY.

Zheng Liu received the B.E. degree in automatic control from the Beijing University of Technology, Beijing, China, in 2016, where he is currently pursuing the Ph.D. degree in control theory and control engineering.

His current research interests include neural networks, intelligent systems, modeling, and control in process systems.

Hongxu Liu received the B.E. degree in control science and engineering from Liaoning Shihua University, Fushun, China, in 2017. He is currently pursuing the Ph.D. degree in control theory and control engineering from the Beijing University of Technology, Beijing, China.

His current research interests include knowledge-based neural-network modeling in complex processes.

Junfei Qiao (Member, IEEE) received B.E. and M.E. degrees in control engineering from Liaoning Technical University, Fuxin, China, in 1992 and 1995, respectively, and the Ph.D. degree in control theory and control engineering from Northeast University, Shenyang, China, in 1998.

From 1998 to 2000, he was a Postdoctoral Fellow with the School of Automatics, Tianjin University, Tianjin, China. He joined the Beijing University of Technology, Beijing, China, where he is currently a Professor. His research interests include neural networks, intelligent systems, self-adaptive/learning systems, and process control systems.

C. L. Philip Chen (Fellow, IEEE) received the M.S. degree in electrical and computer science from the University of Michigan at Ann Arbor, Ann Arbor, MI, USA, in 1985, and the Ph.D. degree in electrical and computer science from Purdue University, West Lafayette, IN, USA, in 1988.

He is the Chair Professor and the Dean of the College of Computer Science and Engineering, South China University of Technology, Guangzhou, China. Being a Program Evaluator of the Accreditation Board of Engineering and Technology Education in the U.S., for computer engineering, electrical engineering, and software engineering programs, he successfully architects the University of Macau's Engineering and Computer Science programs receiving accreditations from Washington/Seoul Accord through Hong Kong Institute of Engineers (HKIE), Hong Kong, which is considered as his utmost contribution in engineering/computer science education for Macau as the former Dean of the Faculty of Science and Technology. His current research interests include cybernetics, systems, and computational intelligence.

Dr. Chen was a recipient of the 2016 Outstanding Electrical and Computer Engineers Award from his alma mater, Purdue University in 1988, after he graduated from the University of Michigan at Ann Arbor in 1985. He received the IEEE Norbert Wiener Award in 2018 for his contribution in systems and cybernetics, and machine learning and two times best transactions paper award from IEEE TRANSACTIONS ON NEURAL NETWORKS AND LEARNING SYSTEMS for his papers in 2014 and 2018. He is also a Highly Cited Researcher by Clarivate Analytics in 2018, 2019, and 2020. He is currently the Editor-in-Chief of the IEEE TRANSACTIONS ON CYBERNETICS, and an Associate Editor of the IEEE TRANSACTIONS ON ARTIFICIAL INTELLIGENCE, and IEEE TRANSACTIONS ON FUZZY SYSTEMS. He was the IEEE Systems, Man, and Cybernetics Society President from 2012 to 2013, the Editor-in-Chief of the IEEE TRANSACTIONS ON SYSTEMS, MAN, AND CYBERNETICS: SYSTEMS from 2014 to 2019. He was the Chair of TC 9.1 Economic and Business Systems of International Federation of Automatic Control from 2015 to 2017. He is a Fellow of AAAS, IAPR, CAA, and HKIE, and a member of Academia Europaea and the European Academy of Sciences and Arts.